

Provided for non-commercial research and educational use only.
Not for reproduction or distribution or commercial use.



Volume 161, Issues 1–2, 1 March 2007

ISSN 0377-0273

Journal of volcanology and geothermal research

An international journal on the geophysical, geochemical, petrological, and economic aspects of geothermal and volcanological research

<http://www.elsevier.com/locate/jvolgeores>



This article was originally published in a journal published by Elsevier, and the attached copy is provided by Elsevier for the author's benefit and for the benefit of the author's institution, for non-commercial research and educational use including without limitation use in instruction at your institution, sending it to specific colleagues that you know, and providing a copy to your institution's administrator.

All other uses, reproduction and distribution, including without limitation commercial reprints, selling or licensing copies or access, or posting on open internet sites, your personal or institution's website or repository, are prohibited. For exceptions, permission may be sought for such use through Elsevier's permissions site at:

<http://www.elsevier.com/locate/permissionusematerial>



ELSEVIER

Available online at www.sciencedirect.com



ScienceDirect

Journal of Volcanology and Geothermal Research 161 (2007) 47–56

Journal of volcanology
and geothermal research

www.elsevier.com/locate/jvolgeores

Development of an ultra-violet digital camera for volcanic SO₂ imaging

G.J.S. Bluth^{a,*}, J.M. Shannon^b, I.M. Watson^c, A.J. Prata^d, V.J. Realmuto^e

^a Department of Geological Engineering and Sciences, Michigan Technological University, Houghton, MI 49931, USA

^b Finlandia University, 601 Quincy Street, Hancock, MI 49930, USA

^c Department of Earth Sciences, University of Bristol, Wills Memorial Building, Queen's Road, Bristol, BS8 1RJ, UK

^d Norwegian Institute for Air Research, P.O. Box 100, Instituttveien 18, NO-2027 Kjeller, Norway

^e Jet Propulsion Laboratory, MS 183-501, 4800 Oak Grove Drive, Pasadena, CA 91109, USA

Received 28 June 2006; received in revised form 27 October 2006; accepted 10 November 2006

Available online 4 January 2007

Abstract

In an effort to improve monitoring of passive volcano degassing, we have constructed and tested a digital camera for quantifying the sulfur dioxide (SO₂) content of volcanic plumes. The camera utilizes a bandpass filter to collect photons in the ultra-violet (UV) region where SO₂ selectively absorbs UV light. SO₂ is quantified by imaging calibration cells of known SO₂ concentrations.

Images of volcanic SO₂ plumes were collected at four active volcanoes with persistent passive degassing: Villarrica, located in Chile, and Santiaguito, Fuego, and Pacaya, located in Guatemala. Images were collected from distances ranging between 4 and 28 km away, with acceptable detection up to approximately 16 km. Camera set-up time in the field ranges from 5–10 min and temporal resolution of up to 6 images per minute is possible, which combined with the camera's field of view makes a continuous SO₂ dataset attainable. Variable in-plume concentrations can be observed and accurate plume speeds (or rise rates) can readily be determined by tracing individual portions of the plume within sequential images.

Initial fluxes computed from camera images require a correction for the effects of environmental light scattered into the field of view. At Fuego volcano, simultaneous measurements of corrected SO₂ fluxes with the camera and a Correlation Spectrometer (COSPEC) agreed within 25%. Experiments at the other sites were equally encouraging, and demonstrated the camera's ability to detect SO₂ under variable background meteorological and environmental conditions. This early work has shown great success in imaging SO₂ plumes and offers promise for volcano monitoring due to its rapid deployment and data processing capabilities, relatively low cost, and improved interpretation afforded by synoptic coverage from a range of distances.

© 2006 Elsevier B.V. All rights reserved.

Keywords: volcano monitoring; ultraviolet camera; degassing; sulfur dioxide

1. Introduction

Establishing baseline sulfur dioxide (SO₂) emissions and interpreting deviations from that baseline is an on-

going objective of volcano hazard monitoring. Changes in SO₂ emissions from background levels can indicate major changes in the volcanic system, often foreshadowing a change in eruptive activity (e.g., Malinconico, 1987; Daag et al., 1996; Gardner and White, 2002). SO₂ is targeted for remote sensing due to its relative abundance in volcanic plumes (2–12% molar mass — Symonds et al., 1994), low

* Corresponding author. Tel.: +1 906 487 3554; fax: +1 906 487 3371.

E-mail address: gbluth@mtu.edu (G.J.S. Bluth).

atmospheric background concentrations (typically less than 10 parts per billion — [Andres and Rose, 1995](#)), and characteristic absorption bands in the ultra-violet (UV) wavelengths ([Millan et al., 1976](#)). Measuring SO₂ emissions from active volcanoes has become a mainstay in monitoring and scientific efforts, since the development of the field-portable correlation spectrometer (COSPEC) in the early 1970s. This paper describes a new ground-based method of imaging and quantifying SO₂ emissions, using a UV camera.

Ground-based SO₂ monitoring has relied primarily on two instruments: COSPEC ([Stoiber et al., 1983](#)) and, more recently, compact UV spectrometers adapted for ground-based monitoring, collectively referred to here by the retrieval technique employed — DOAS (Differential Optical Absorption Spectroscopy; e.g., [Galle et al., 2003](#)). These instruments use scattered sunlight as the UV light source, and take advantage of selective absorption of UV light by SO₂ ([Moffat and Millan, 1971](#); [Millan et al., 1976](#); [Platt, 1994](#)). Transects of the emitted plume are taken either from a fixed position by rotating the instrument, or by keeping the sensor stable and scanning through the plume by means of automobile, boat, or aircraft traverses. SO₂ fluxes are thereby derived from the measured cross-sectional burden and the plume speed. COSPEC and DOAS field campaigns during periods of volcanic unrest have significantly advanced our understanding of eruption processes and pre-eruption monitoring (e.g., [Symonds et al., 1994](#); [Stix and Gaonac'h, 2000](#); [Edmonds et al., 2003a,b](#)).

However, there are significant limitations to scanning techniques. For example, the wind speed calculation can contribute up to 40% to the overall error ([Casadevall et al., 1981](#); [Stoiber et al., 1983](#)), as it must be derived independently from hand-held devices or local weather stations that may or may not represent the wind profile at the actual plume height and location. Measuring plumes with multiple instruments can reduce this problem significantly ([McGonigle et al., 2005](#); [Williams-Jones et al., 2006](#)). The field of view is relatively small for COSPEC and compact UV spectrometers, and the data represent a localized cross-section of the moving plume averaged over the duration of the scan. Therefore variations in plume composition during the scan, or flux changes occurring faster than the sampling rate, cannot be recognized. Fluctuations in calculated emission rates can result from changes in meteorological conditions and/or changes in subsurface magmatic processes or interactions. In addition, SO₂ begins to disperse and chemically convert to sulfuric acid aerosol immediately upon entering the atmosphere ([Eatough et al., 1994](#)), and down-wind measurements may therefore progressively underestimate

the actual emission rates. However, [McGonigle et al. \(2004\)](#) found negligible impacts from SO₂ removal on flux calculations downwind of Masaya volcano, Nicaragua.

Thus, scanning method limitations can seriously impact two common objectives of SO₂ monitoring: (1) the need to collect continuous, accurate data for an extended period of time; and (2) the need to identify and evaluate emission fluctuations. Measured SO₂ emissions may vary due to volcanic processes, or as a result of inhomogeneous mixing caused by physical and chemical dispersion processes in the atmosphere. During a volcanic process it is difficult to evaluate changes in SO₂ degassing based upon sporadic measurements, or compare these sporadic SO₂ emission rate estimates to continuous measurements such as seismicity or ground deformation (see [Edmonds et al., 2003b](#), which describes a continuous scanning system employed at Montserrat to compare relatively high-speed [10 measurements per hour] SO₂ measurements to seismic data).

Significant improvements to volcanic SO₂ monitoring may be possible through imaging, which ideally captures a large extent of a volcanic plume in a single image and maps the spatial variations in SO₂ content. UV satellite-based imaging of volcanogenic SO₂ has successfully monitored large-scale volcanic activity for over 25 years, and the most advanced system to date, OMI (Ozone Monitoring Instrument), can produce daily global SO₂ maps at 13 × 24 km² nadir resolution ([Krotkov et al., 2006](#)). [Nguyn et al. \(1995a,b\)](#) developed a method of UV imaging of SO₂ pollution plumes in the laboratory, using optical interferometry and a CCD detector. [Sandsten et al. \(1996\)](#) also created a laboratory technique to image gas plumes by gas-correlation spectrometry (comparison of measured plume absorption to that of calibration cells) in the infrared. [Bobrowski et al. \(2006\)](#) have developed an imaging DOAS method capable of scanning through a complete plume to produce a gas distribution map of SO₂ and several other gases, at a rate of approximately 15 min per image.

This research is based on a UV instrument concept that was tested at NASA's Jet Propulsion Laboratory, which showed that the digital response of a gas filter camera was proportional to the line-of-sight burden of SO₂ ([Realmuto, 1998](#)). We describe the basics of a newly-developed UV camera system, which builds upon many aspects of previous imaging efforts, and the first field tests conducted at four active volcanoes in South and Central America in 2004–2005.

2. Methods and materials

Instrumentation includes an Apogee Instruments E6 Alta digital camera with a Kodak KAF-1001E-2

1024×1024 CCD array with 16-bit quantization level per pixel, a 105 mm lens from Coastal Optics, and a bandpass filter from Andover Optics centered at 307 nm with a 12 nm full width half max bandwidth, mounted on a standard camera tripod, and powered by two dry cell 6 volt batteries (Fig. 1). The total cost for these components was less than \$18,000 (2005 prices). Camera operation is controlled by a laptop computer with MaxIm DL computer software (by Diffraction Limited; included with the digital camera) via an Ethernet cable. The CCD includes a thermo-electric cooler and fan system, but our tests found that the CCD dark current remained below background noise of the camera with only the fan in use.

Field set-up time is approximately 5–10 min and includes taking sample images of the plume to adjust focus and exposure time. Focus is adjusted manually by using the top of the volcano as a target. The camera's field of view (FOV) is approximately 13° (~5 m resolution pixels at 10 km range), which provides a relatively large image of an emitted gas plume (see Figs. 2–5). Exposure time is adjusted to produce the best separation of plume from background without pixel saturation (typical midday exposure times are 0.5–0.8 s). Two fused-silica calibration cells, made by Resonance Ltd., provided SO₂ concentration-pathlength products of 115 and 270 ppm m, respectively. These cells have flat absorption within 1% in the 290–320 nm spectral range, and were imaged before, after, and roughly every 60 minutes during data collection, although no evidence of instrument response drift was observed during our field tests.

Field measurement sites were selected to optimize plume imaging, similar to criteria used for scanning



Fig. 1. Field set-up of UV camera and associated components. The camera and lens are mounted on a tripod, and connected to the laptop computer (kept under the towel, due to glare). The laptop and camera are powered by two 6-volt batteries, although other power sources are possible.

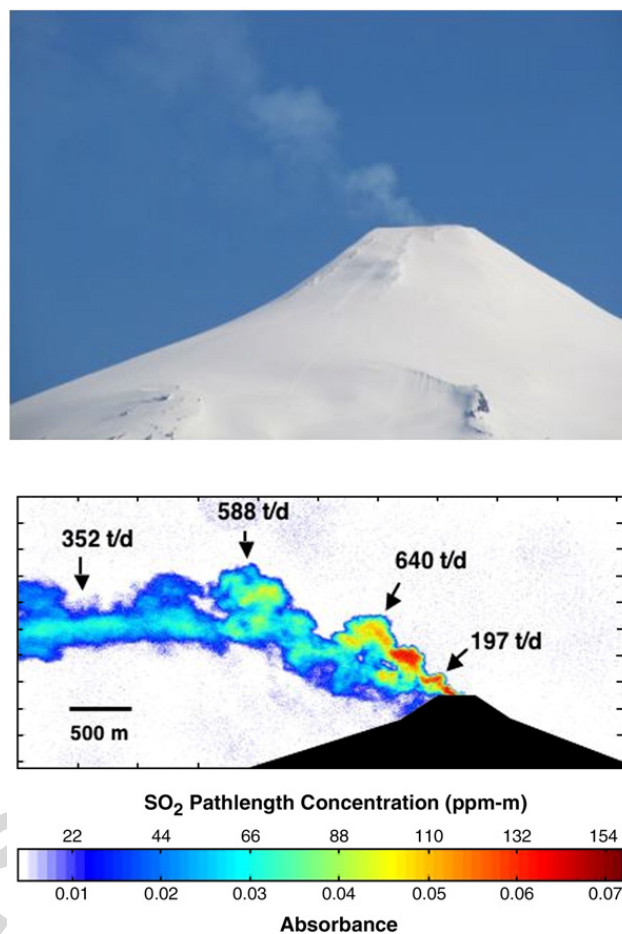


Fig. 2. a) Visible image of Villarrica taken with a digital camera from a distance of 16.5 km. b) Near-simultaneous image of Villarrica taken from the same location but using the UV camera, with a 0.8 s exposure, to discriminate SO₂. Plume absorbances are scaled to calibration cell results. A wind speed of 4.5 m s⁻¹ was calculated from measuring movement of distinctive portions of the plume on consecutive images. Fluxes are calculated on different portions of the plume using an air light correction (see text), with arrows indicating the cross-sectional slice orientation (t/d = tonnes per day). The faded blue circles are a result of particles or spots on the camera optics.

spectrometer placements: (1) the camera viewing direction is near perpendicular to plume direction; (2) a sufficient area of open sky is available as background; and (3) the sun is directly overhead or behind the camera viewing direction. In the field, a cardboard collimator is used to reduce the amount of direct and scattered light on the lens; therefore keeping the sun behind the camera reduces background noise, but is not a necessity for imaging.

An SO₂ slant column density map is generated from the raw image. The background sky values are averaged to eliminate vignetting — a condition where light intensity decreases toward the edges of the image. Most vignetting is an optical effect observed with longer lenses in which oblique light does not illuminate the image corners. The MaxIm software includes an interactive routine which

employs user-selected points to recalculate the background sky to nearly uniform light intensity throughout the image. This algorithm does not significantly change the magnitude of the plume to background ratio. The absorbance in each plume pixel is computed by comparing plume pixels with the average background, using the relationship

$$A = \log_{10}(I_o/I) \quad (1)$$

where I_o = light intensity before passing through SO_2 (background sky), and I = light intensity after passing through SO_2 . The plume absorbances are then scaled to concentration-pathlength products using measured calibration cell absorbances, to derive an SO_2 slant column concentration for any plume pixel.

The dimensions of a pixel in a given UV camera image can be easily calculated, knowing the size and dimension of the CCD array, the focal length of the lens, and measuring the distance from the camera to the target (Shannon, 2006). Plume velocity is thereby calculated directly by measuring the distance traveled of distinctive plume features on consecutively timed images; however,

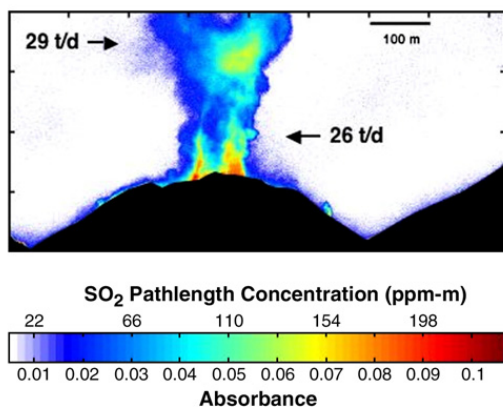
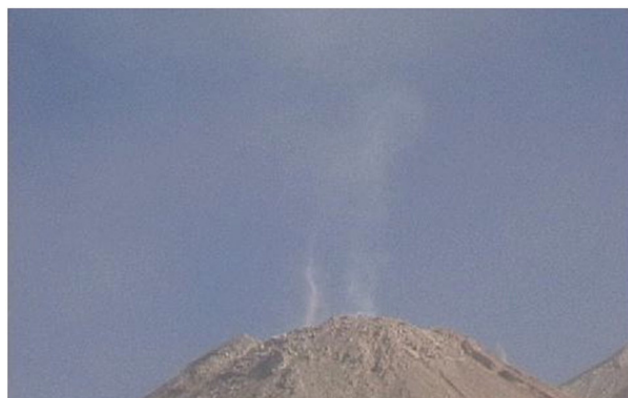


Fig. 3. a) Visible still image of Santiaguito plume collected from video camera footage. b) UV camera image of Santiaguito SO_2 plume collected at the same location and time using a 0.5 s exposure time. Flux calculations and plume absorbance characteristics as explained in Fig. 2.

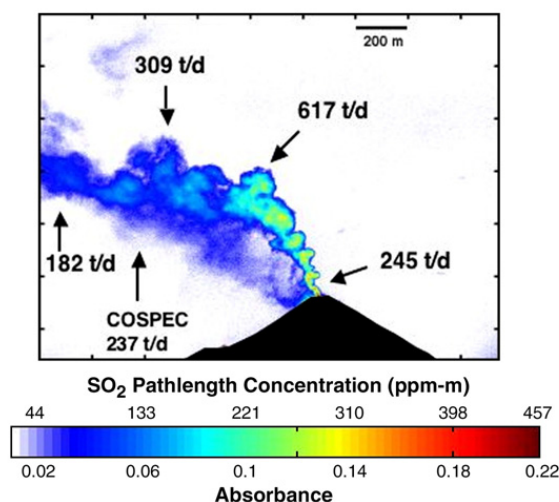
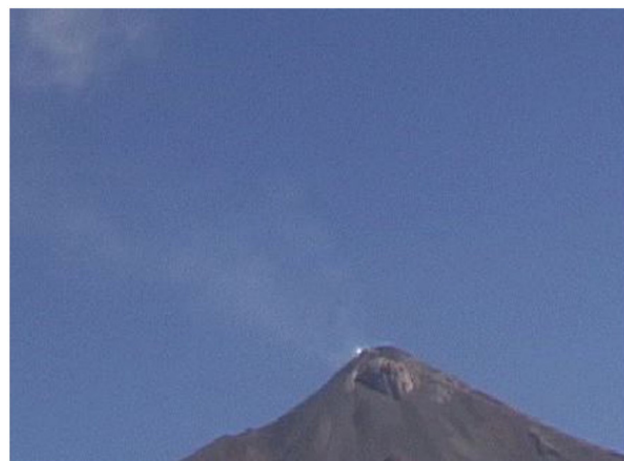


Fig. 4. a) Visible still image of the Fuego plume collected from video camera footage from 7.08 km distance. b) simultaneous UV camera image of Fuego SO_2 plume taken at the same location and time using 0.5 s exposure. Flux calculations and plume absorbance characteristics as explained in Fig. 2.

wind direction must be determined independently for drifting plumes. SO_2 fluxes can be calculated similarly to scanning methods, by integrating the abundance over transects (correcting, as needed, for non-perpendicular plume viewing angles) and multiplying the integrated mass by the plume velocity. As the camera FOV covers a broad section of plume, multiple cross-sections (or areas) can be evaluated to eliminate problems from plume heterogeneity.

3. Results

We were able to test the camera under a variety of field conditions, with variations in emission levels, distance from the volcano, atmospheric and meteorological conditions, and plume geometries, similar to what would be expected in a volcano monitoring program. For the

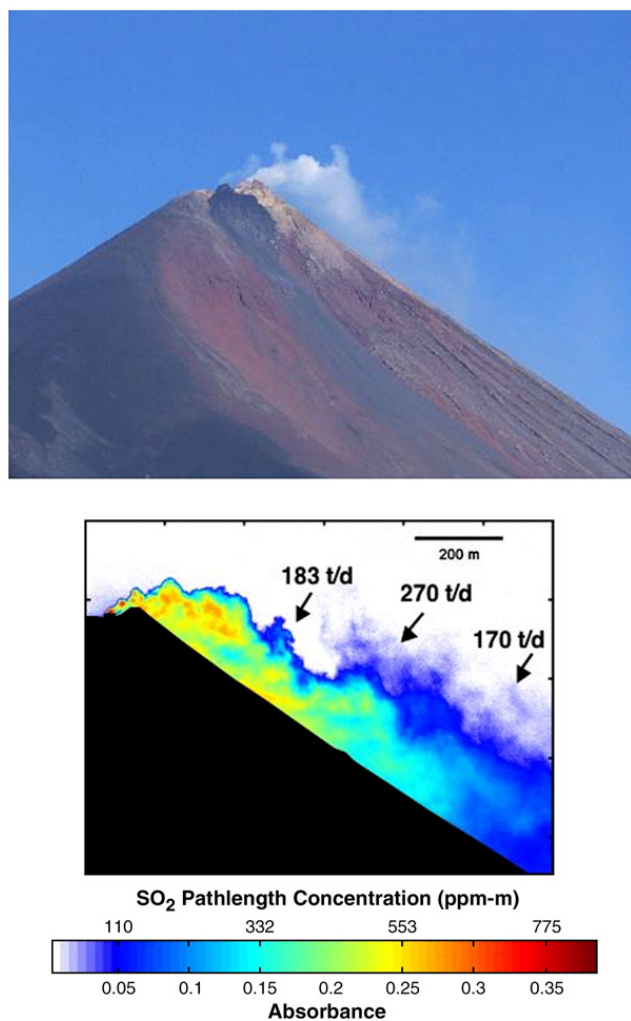


Fig. 5. a) Visible image of Pacaya volcano taken just prior to the UV camera sequence. b) the Pacaya SO₂ plume collected from 3.64 km with a 0.5 s exposure. Flux calculations and plume absorbance characteristics as explained in Fig. 2.

purpose of demonstrating this technique, cloud-free images are displayed for each field site. Many images were taken under conditions with significant meteorological clouds. Clouds behind the plume produced no significant effect on SO₂ retrievals compared to clear-sky backgrounds. Meteorological clouds between the camera and plume affected the SO₂ retrievals, as would be the case for scanning methods. However, even if the field of view is partially obscured by meteorological clouds, it is possible to derive SO₂ fluxes from the cloud-free regions of the UV camera image.

3.1. Villarrica

Villarrica volcano is a basaltic–andesitic stratovolcano, located in southern Chile (39.42° S, 71.93° W), with a summit height of 2850 m. Volcanic activity consisted

of a persistent gas plume emanating from the lava lake. Visible and UV images of Villarrica were collected on November 17–18, 2004 from four different locations ranging from approximately 8–20 km from the volcano. At these distances, pixel resolutions ranged from 1.92 m to 4.79 m, respectively. Meteorological conditions during this period ranged from cloud-free, to abundant; meteorological clouds in the background had virtually no effect on SO₂ discrimination.

Fig. 2 compares a visible and false color ultraviolet image of the Villarrica plume taken coincidentally from 16.5 km N of the volcano. The clean, cloud-free atmosphere provided an ideal background, and absorption of UV light by SO₂ in the volcanic plume allows distinct discrimination from the background sky. The SO₂ plume demonstrates significant heterogeneity; calculated fluxes ranged over at least a factor of three in this plume image, which might be difficult to resolve using a scanning technique.

3.2. Santiaguito

Santiaguito volcano is a dacitic lava dome located on the WNW-trending volcanic front in Guatemala (14.756° N, 91.552° W). The SO₂ plume was imaged with the UV camera on January 17, 2005 from 4.12 km S of the volcano. Activity during this time period consisted of a continuous gas plume interspersed with moderately sized, ash-rich vulcanian eruptions every 0.5–2 h. Images were collected in the mid-morning; low-level clouds typically form daily by noon and obscure the top of the dome.

Fig. 3a shows a (visible) photograph of the Santiaguito dome on the morning of January 17, 2005 collected from a video camera and Fig. 3b shows a coincidental image taken with the UV camera using a 0.5 s exposure time. Imaging conditions were challenging at Santiaguito; the frequent explosions produced small amounts of ash and steam that lingered several hundred meters above the Santiaguito dome for several minutes to hours due to calm wind conditions. These constituents can absorb and/or scatter UV light and interfere with SO₂ retrievals (Krotkov et al., 1997). To reduce their interference, only a small portion of plume extending to approximately 200 m above the vent was used for analysis, resulting in consistent flux determinations. While water vapor is a major constituent of volcanic plumes SO₂ is a much stronger absorber in the 300–320 nm range, which allows for resolution of the SO₂ component in UV scanning or imaging methods. The pixel resolution from this location is ~1 m per pixel and a time series of images was used to calculate a plume rise rate of 5.5 m.

3.3. Fuego

Fuego is a basaltic stratovolcano located on the WNW trending volcanic front in Guatemala (14.473° N, 90.880° W) with a summit elevation of 3763 m. Activity consisted of a continuous gas plume interrupted by infrequent periods of more intense puffing and small, relatively ash-free, eruptions. Images of the Fuego SO₂ plume were collected during January 18–20, 2005 from five different locations ranging from approximately 7 to 28 km distance (close to the maximum distance where a plume could still be resolved). Visible air quality was hindered locally by wind-driven dust, as well as vehicle-generated dust and particulates from the burning of sugar cane fields.

Fig. 4a shows a still image of the Fuego plume acquired from video camera footage in the visible compared to a simultaneous image collected with the UV camera (Fig. 4b) from 7.08 km SW. The UV image was acquired using a 0.5 second exposure. The pixel resolution is 1.7 m per pixel, and the image-determined plume speed was 4.6 m s⁻¹. The cloudless conditions provide uniform and consistent illumination, and the SO₂ plume is detected with remarkable detail and displaying a range of dynamics in plume dispersal. Fluxes ranged over at least a factor of three within the plume image. With the exception of fluxes calculated immediately above the vent, flux values decrease with distance from the volcano and suggest that the SO₂ plume is dispersing below detection limits downwind as the plume mixes with the ambient atmosphere.

3.4. Pacaya

Pacaya is a basaltic cone located on the WNW trending volcanic front in Guatemala (14.381° N, 90.601° W) with a summit elevation of 2552 meters. Images of the Pacaya SO₂ plume were collected on January 20, 2005 from 3.64 km W. Frequent lava spattering could be observed at the summit during this time period along with a persistent, water-rich gas plume. During our image collection period, the plume hugged the downwind (south) slope of the cone.

Fig. 5a shows a visible image of the Pacaya cone and gas plume, and Fig. 5b shows the UV camera image taken minutes afterward, using an exposure time of 0.5 s. The pixel resolution is 0.87 m per pixel. A plume speed of 7.7 m s⁻¹ was computed from subsequent images.

Fluxes calculated at various locations within a single plume image exhibit large variability. This variability has been observed at all the test volcanoes, especially Villarrica and Fuego. A possible explanation for the variability observed at Pacaya may lie in turbulence

effects that concentrate parts of the plume resulting in pockets of higher SO₂. As the plume spills down the leeward side of the cone, the surface causes turbulent eddies in the wind field. The fluxes calculated represent minimum values, because the lower boundary of the plume is assumed to be the boundary where it meets the volcano flank. However, some portions of the plume may not be included in the cross-section since not all of the plume may be visible to the camera (some portions may have drifted behind or in front of the flank).

4. Discussion

The four volcanoes used as initial test sites for the UV camera provided diverse field conditions to evaluate the camera's effectiveness for volcanic SO₂ monitoring. The camera proved to be especially practical and efficient to operate in the field. Set-up time is less than 10 min and several dozen images can be collected in under a half-hour. The camera system, laptop and batteries are light enough to be brought to a site by backpack. A map of SO₂ abundance can be prepared in about 5 minutes, and a (uncorrected) flux can be quickly computed using plume speeds derived from a sequence of several images. Thus, the camera has the capability to be deployed quickly, and detect rapid changes in SO₂ fluxes, as well as day to day monitoring tasks.

The camera CCD and optics are sensitive to the ambient light intensity conditions, and therefore to sun angle and scattered light from surrounding objects (i.e. trees, soil, structures, etc.). Image quality (clarity, background homogeneity) is best with the sun opposite the imaging direction (behind the operator). For each site, with unique conditions of sun angle, background sky conditions and light levels, it was necessary to adjust exposure time to maximize the plume separation from background.

The camera was able to produce images of the SO₂ plumes from distances of 4 to 28 km. Obviously, atmospheric and plume conditions will affect the quality of the images, but in the case of Villarrica with a significant SO₂ plume and, clear atmospheric conditions, high-quality detection was obtained at a distance of 16 km. Our field tests of camera-plume distances versus image quality suggest 5–10 km distance is optimum, providing many siting options for volcano monitoring considering both safety and viewing ability (balancing resolution and sufficient FOV). The detection distance, and consequently view angle, is also important considering that fixed-base scanning and imaging techniques measure “slant columns” through the plume, which represent SO₂ amounts measured at viewing angles inclined from zenith (i.e. not

“vertical columns”, which is how traverse measurements and satellite SO₂ data are reported) and need to be converted to vertical columns to produce consistent measurements (e.g., Edmonds et al., 2003a).

Our tests demonstrated that the UV camera could easily detect SO₂ plumes, but our initial SO₂ flux calculations were more than an order of magnitude below those calculated for coincident COSPEC measurements (Table 1). We performed a set of field tests at Fuego volcano, in which we observed that the plume “contrast”, or the percentage difference between target and background luminance (McCartney, 1976), decreased exponentially with distance. In other words, the plume signal becomes brighter (i.e. the plume absorbance decreases) with distance while the background level stays relatively the same. Through the absorbance and Beer’s Law relationships, lower plume absorbance translates to a lower estimate of SO₂ abundance and, consequently, an artificially lower mass flux.

The cause for the exponential reduction in contrast between the plume and the background with increasing distance is due to molecular scattering (proportional to λ^{-4} , hence much more significant at UV wavelengths). The source of light can be directly scattered sunlight, diffuse skylight, and ground-reflected light. The true/attenuated contrast is an exponential function of the distance and the wavelength-dependent volume scattering coefficient of the atmosphere (McCartney, 1976). In the UV, scattering of radiation by air molecules is an order of magnitude larger than in the visible spectrum (Penndorf, 1957). Mori et al. (2006) found that this effect, in the 309–315 nm range, became significant at 1.5 km distance, and caused up to 50% underestimation of fluxes at the shorter wavelengths.

Moffat and Millan (1971) describe a correction for the effects of “dilution light” (i.e., molecular scattering) on COSPEC data (more modern COSPEC instruments have automatic gain control to deal with changes in background illumination and contrast). Similarly, we devel-

oped an empirical atmospheric scattering correction scheme (Appendix 1; after Shannon, 2006).

With the exception of Santiaguito, applying the scattering correction resulted in fluxes that more closely matched the results of COSPEC or values more commonly measured at that particular volcano (Table 1). At Villarrica, the correction produced an order of magnitude increase, from 21 t/day to a corrected flux of 352 t/day on the least turbulent part of the plume, or an average of 444 t/day using all four measurements (Fig. 2b). The corrected fluxes fall between the 260 t/day measured in 2000 (Witter et al., 2000) and the 460 t/day measured in 2001 (Witter et al., 2001) at Villarrica using COSPEC under open-vent conditions, similar to those observed during our campaign. We also had access to a DOAS instrument at the 16.5 km distance site, but it was unable to discriminate the SO₂ plume from background at that distance (L. Rodriguez, personal communication 2004).

At Santiaguito, correcting for scattering results in a flux of 26 t/day directly over the vent (Fig. 3b). Coincidental COSPEC measurements produced an average flux of 160 t/day using a wind speed of 3.5 m s⁻¹ derived from a meteorological station at the nearby Santiaguito observatory (G. Chigna, personal communication 2005). However, COSPEC measurements targeted the plume where it stopped rising and began to drift horizontally, rather than in the vertical-rising part of the plume where the UV camera fluxes were calculated. On that morning, the plume stagnated and spread at an altitude approximately 600–800 m above the vent. We suspect that the pooling of the plume artificially inflated the COSPEC SO₂ results. It is worth noting that COSPEC SO₂ measurements collected in 2002 under similar volcanological conditions, but more active wind conditions, ranged from 20–190 t/day (Rodriguez et al., 2004).

At Fuego volcano, applying the scattering correction produced a flux of 309 t/day approximately 600 m downwind of the vent (Fig. 4b). Coincidental COSPEC

Table 1
UV camera field test results: SO₂ fluxes

	Villarrica (t/day)	Santiaguito (t/day)	Fuego (t/day)	Pacaya (t/day)
Measurement date	Nov 17, 2004	Jan 17, 2005	Jan 18, 2005	Jan 20, 2005
UV camera (uncorrected)	21	10	34	127
UV camera (corrected)	352	26	309	270
COSPEC-derived fluxes	260, 460 ^a	210 ^b	237 ^b	300–400 ^c
Field observations	Clear, clean atmosphere	Sensors measured different plume regions	Both sensors measured same location	Plume hugging flank

^a Data from 2000 (Witter et al., 2000) and 2001 (Witter et al., 2001).

^b Simultaneous measurements of UV camera and COSPEC.

^c Range of measurements from the previous 6 months (G. Chigna, personal communication 2005).

measurements report 237 t/day using a wind speed of 5 m s⁻¹ derived from a meteorological station located on neighboring Agua volcano, 20 km E (G. Chigna, personal communication 2005). The COSPEC transect location was similar to those measured in the UV camera image, and the COSPEC flux represents an average of measurements collected for about one hour surrounding this time. The work at Fuego produced the most robust comparisons, considering the near-simultaneous measurements, and similar scanning region of the emitted plume, thus it is encouraging that the flux results were similar.

At Pacaya, condensed water droplets observed in the plume may affect SO₂ retrievals by absorbing or scattering UV light, so fluxes were computed in portions of the plume further downwind of the vent (>300 m) where most of the water appeared to have evaporated; the corrected SO₂ fluxes were 270 t/day about 400 m down the flank. No coincidental measurements of COSPEC or DOAS were possible due to the difficult viewing conditions, but our results are similar to COSPEC measurements within the previous 6 months of 300–400 t/day (G. Chigna, personal communication 2005). This example also shows that plume fluxes can be derived even when a plume-free portion of the sky is not available on both sides of the plume — a necessity relied upon for COSPEC and DOAS measurements.

The simple scattering correction allows us to quantify SO₂ fluxes for the purposes of testing the utility of the camera, but more experiments are needed to validate the method. With the current broad-band filter approach, a scattering correction would be needed for each field situation. Continuing work focuses on the effects of atmospheric opacity on camera response, incorporation of additional, narrow-band UV camera filters (e.g., as with satellite instruments such as OMI, reducing atmospheric interference by using band ratios within the SO₂ absorption spectrum; Krotkov et al., 2006), as well as radiative transfer modeling to properly assess camera response.

5. Conclusions

We have successfully field-tested a digital ultraviolet camera to take images of passive volcanic SO₂ plumes. At a distance of 5–10 km, the camera provides a FOV of several square kilometers, with pixel resolutions of approximately 1–2 m, respectively. Calibrated images show significant variations in plume abundance, providing a means for evaluating physical and chemical dispersion processes in the plume. Consequently, portions of the plume can easily be tracked in timed image sequences that allow accurate plume velocities to be calculated directly. Measured plume absorbances are scaled to concentration-pathlength products using calibration cell measurements,

to derive an SO₂ slant column concentration for any plume pixel, and SO₂ fluxes can be derived using measured plume speeds. The camera's current ability to produce accurate SO₂ fluxes requires significant additional work to characterize the local environmental conditions (e.g., wind direction, atmospheric scattering effects).

Field studies were undertaken at four different volcanic settings, providing a good test of the camera under potential monitoring conditions. Volcanic SO₂ plumes were detected at distances ranging from about 3 to 28 km. Because the plume signal decreases with distance, scattered light by the intervening atmosphere is suspected to dilute the plume signal, reducing plume-background contrast, and cause an overall underestimate of plume concentrations. A scattering correction was applied to subtract the effects of light scattering — since we use a single, broad-band UV filter for this stage of the camera development, using a DOAS technique was not possible. Alternatively, more expensive narrow-band filters could be used to match SO₂ absorption peaks in the 300–320 nm range.

The most robust evaluation of the camera was at Fuego volcano, where simultaneous COSPEC and corrected UV camera SO₂ fluxes, using the same portions of the plume, agreed to within 25%. At Villarrica, results were within the range of recent COSPEC measurements under similar activity levels. At Pacaya, the UV camera fluxes were slightly less than recent COSPEC measurements, but the plume was hugging the volcano flank and was not fully visible. At Santiaguito volcano, the UV camera fluxes taken just above the vent were well below those of the COSPEC measurements, which scanned a portion of the plume where we suspect the SO₂ “pooled” under stagnant wind conditions.

The camera images demonstrate considerable heterogeneity in all of the plumes owing either to emission variations or turbulence. The ability to determine the cause of flux variations by direct observation and interpretation of a plume concentration map is a major step forward in volcano gas monitoring. Future work will concentrate on accurate camera calibration under laboratory as well as a variety of environmental and volcanological conditions. The UV camera holds great promise as a future SO₂ monitoring instrument due to its quick set-up, practical field use, timely processing of results, and relatively low cost.

Acknowledgements

Funding for this research was provided by the National Science Foundation through EAR-0337120 to GJSB and EAR-0321869 to IMW. We appreciate Guatemalan field support from Gustavo Chigna of INSIVUMEH. This

paper is based upon the Ph.D. research of JMS with many useful suggestions by W. Rose and R. Shaw. This manuscript benefited greatly from thorough reviews by Simon Carn and an unidentified reviewer.

Appendix A. Correction procedure for atmospheric scattering

1. Plume contrast is computed from the following equation (after McCartney, 1976):

$$C = \frac{L_o - L_b}{L_b} \quad (2)$$

where C =contrast, L_o =object (plume) luminance, and L_b =background luminance.

The luminance is simply the brightness value recorded by the camera CCD.

2. A set of plume measurements at different camera-target distances is used to construct a contrast attenuation curve. The attenuation of this contrast with distance is defined as:

$$C_R = C_0 \exp(-\beta R) \quad (3)$$

where C_R =apparent contrast at distance R , C_0 =true contrast at zero distance, β =volume scattering coefficient, and R =distance between object and observer.

3. Eq. (3) is fit to the distance-contrast data to estimate C_0 , the zero-distance (zero-scattering) plume contrast, and β , which describes the degree to which a volume of air can scatter light per unit distance, defined for both molecules and particles. At 310 nm in the ultra-violet (nearest our 307 nm filter), β is approximately 0.125 km^{-1} for pure air (Penndorf, 1957). For the Fuego volcano field measurements, β was determined to be 0.2 km^{-1} , suggesting that the atmosphere here was less clear.

4. The corrected plume contrast can then be used to calculate a new plume absorbance. Recall that (uncorrected) plume absorbances are calculated using Eq. (1), from an average plume and average background signal. To calculate a *new* plume signal, the average background value and the new zero-scattering plume contrast are entered into the plume contrast Eq. (2) and solved for the new average plume signal ($L_{o, \text{new}}$).

5. The difference ($L_{o, \text{diff}} = L_{o, \text{new}} - L_o$) between the old and new average plume signal is the scaling factor used to reduce each plume pixel value, and calculate the new average plume cross-section. This new adjusted average plume cross-section value is then used in Eq. (1) to calculate a new cross-sectional average plume absorbance.

6. This new average cross-sectional absorbance is scaled to the calibration cells to convert to ppm m, and an atmospheric scattering corrected flux.

References

- Andres, R.J., Rose, W.I., 1995. Remote sensing spectroscopy of volcanic plumes and clouds. In: McGuire, B., Kilburn, C.R.J., Murray, J. (Eds.), *Monitoring Active Volcanoes*. University College London Press, pp. 301–314.
- Bobrowski, N., Hönninger, G., Lohberger, F., Platt, U., 2006. IDOAS: a new monitoring technique to study the 2D distribution of volcanic gas emissions. *Journal of Volcanology and Geothermal Research* 150, 329–338.
- Casadevall, T.J., Johnston, D.A., Harris, D.A., Rose Jr., W.I., Malinconico Jr., L.L., Stoiber, R.E., Bornhorst, T.J., Williams, S.N., Woodruff, L., Thompson, J.M., 1981. SO₂ emission rates at Mount St. Helens from March 29 through December 1980. In: Lipman, P.W., Mullineaux, D.R. (Eds.), *The 1980 Eruptions of Mount St. Helens*. U.S. Geological Survey Professional Paper, vol. 1250, pp. 193–200.
- Daag, A.S., Tubianosa, B.S., Newhall, C.G., Tungol, N.M., Javier, D., Dolan, M.T., Reyes, P.J.D., Arboleda, R.A., Martinez, M.M.L., Regalado, M.T.M., 1996. Monitoring Sulfur Dioxide Emission at Mount Pinatubo, in Newhall, C.G. and Punongbayan, R.S. (Eds.), *Fire and Mud: Eruptions and Lahars of Mount Pinatubo, Philippines*, Philippine Institute of Volcanology and Seismology, Quezon City, and University of Washington Press, Seattle, 409–414.
- Eatough, D.J., Caka, F.M., Farber, R.J., 1994. The conversion of SO₂ to sulfate in the atmosphere. *Israel Journal of Chemistry* 34, 301–314.
- Edmonds, M., Herd, R.A., Galle, B., Oppenheimer, C.M., 2003a. Automated, high time-resolution of SO₂ flux at Soufrière Hills Volcano, Montserrat. *Bulletin of Volcanology* 65, 578–586.
- Edmonds, M., Oppenheimer, C.M., Pyle, D.M., Herd, R.A., Thompson, G., 2003b. SO₂ emissions from Soufrière Hills Volcano and their relationship to conduit permeability, hydrothermal interaction and degassing regime. *Journal of Volcanology and Geothermal Research* 124, 23–43.
- Galle, B., Oppenheimer, C., Geyer, A., McGonigle, A., Edmonds, M., 2003. A mini-DOAS spectrometer in remote sensing of volcanic SO₂ emissions. *Journal of Volcanology and Geothermal Research* 119, 241–254.
- Gardner, C.A., White, R.A., 2002. Seismicity, gas emission and deformation from 18 July to 25 September 1995 during the initial phreatic phase of the eruption of Soufrière Hills Volcano, Montserrat. In: Druitt, T.H., Kokelaar, B.P. (Eds.), *The Eruption of Soufrière Hills Volcano, Montserrat, from 1995 to 1999*. . *Memoirs*, vol. 21. Geological Society, London, pp. 567–581.
- Krotkov, N.A., Krueger, A.J., Bhartia, P.K., 1997. Ultraviolet optical model of volcanic clouds for remote sensing of ash and sulfur dioxide. *Journal of Geophysical Research* 102, 21891–21904.
- Krotkov, N.A., Carn, S.A., Krueger, A.J., Bhartia, P.K., Yang, K., 2006. Band residual difference algorithm for retrieval of SO₂ from the AURA Ozone Monitoring Instrument (OMI). *IEEE Transactions on Geoscience and Remote Sensing* 44, 1259–1266.
- Malinconico Jr., L.L., 1987. On the variation of SO₂ emission from volcanoes. *Journal of Volcanology and Geothermal Research* 33, 231–237.
- McCartney, E.J., 1976. *Optics of the Atmosphere*. John Wiley & Sons, Inc., pp. 34–44.
- McGonigle, A.J.S., Delmelle, P., Oppenheimer, C., Tsanev, V.I., Delfosse, T., Williams-Jones, G., Horton, K., Mather, T.A., 2004. SO₂ depletion in tropospheric volcanic plumes. *Geophysical Research Letters* 31. doi:10.1029/2004GL019990.
- McGonigle, A.J.S., Hilton, D.R., Fischer, T.P., Oppenheimer, C., 2005. Plume velocity determination for volcanic SO₂ flux measurements. *Geophysical Research Letters* 32. doi:10.1029/2005GL022470.

- Millan, M.M., Gallant, A.J., Turner, H.E., 1976. The application of correlation spectroscopy to the study of dispersion from tall stacks. *Atmospheric Environment* 10, 499–511.
- Moffat, A.J., Millan, M.M., 1971. The applications of optical correlation techniques to the remote sensing of SO₂ plumes using sky light. *Atmospheric Environment* 5, 677–690.
- Mori, T., Mori, T., Kazahaya, K., Ohwada, M., Hirabayashi, J., Yoshikawa, S., 2006. Effect of UV scattering on SO₂ emission rate measurements. *Geophysical Research Letters* 33. doi:10.1029/2006GL026285.
- Nguyn, C.T., Galais, A., Fortunato, G., 1995a. Pollution imagery by optical interferometry: application to SO₂ gas. *Applied Optics* 34, 5398–5405.
- Nguyn, C.T., Journet, B., Fortunato, G., 1995b. Description of an acquisition unit for optical interferometry treatment: application to the pollution imagery of SO₂ gas. *Review of Scientific Instruments* 66, 5183–5191.
- Penndorf, R., 1957. Tables of the refractive index for standard air and the Rayleigh scattering coefficient for the spectral region between 0.2 and 20.0 μm, and their application to atmospheric optics. *Journal of the Optical Society of America* 47, 176–182.
- Platt, U., 1994. Differential optical absorption spectroscopy (DOAS). In: Sigrist, M.W. (Ed.), *Air monitoring by spectroscopic techniques*. Wiley, Chichester, pp. 27–84.
- Realmuto, V.J., 1998. Final Report: Imaging Gas Correlation Camera. Contract NAS7-1260, Task Order RF152, Amendment 0778, NASA Jet Propulsion Laboratory.
- Rodriguez, L.A., Watson, I.M., Rose, W.I., Branan, Y.K., Bluth, G.J.S., Chigna, G., Matías, O., Escobar, D., Carn, S.A., Fischer, T.P., 2004. SO₂ emissions to the atmosphere from active volcanoes in Guatemala and El Salvador, 1999–2002. *Journal of Volcanology and Geothermal Research* 138, 325–344.
- Sandsten, J., Edner, H., Svanberg, S., 1996. Gas imaging by infrared gas-correlation spectrometry. *Optics Letters* 21, 1945–1947.
- Shannon, J.M., 2006. Development and application of new techniques for sulfur dioxide monitoring at active volcanoes. Ph.D. dissertation, Michigan Technological University.
- Stix, J., Gaonac'h, H., 2000. Gas, plume and thermal monitoring. *Encyclopedia of Volcanoes*. Academic Press, pp. 1141–1163.
- Stoiber, R.E., Malinconico Jr., L.L., Williams, S.N., 1983. Use of the correlation spectrometer at volcanoes. In: Tazieff, H., Sabroux, J.C. (Eds.), *Forecasting Volcanic Events*, pp. 425–444. Amsterdam-New York.
- Symonds, R.B., Rose, W.I., Bluth, G.J.S., Gerlach, T.M., 1994. Volcanic-gas studies: Methods, results, and applications. In: Carroll, M.R., Holloway, J.R. (Eds.), *Volatiles in Magmas*. *Reviews in Mineralogy*, vol. 30, pp. 1–60.
- Williams-Jones, G., Horton, K.A., Elias, T., Garbeil, H., Mouginiis-Mark, P.J., Sutton, A.J., Harris, A.J.L., 2006. Accurately measuring volcanic plume velocity with multiple UV spectrometers. *Bulletin of Volcanology* 68, 328–332.
- Witter, J.B., Kress, V.C., Calder, E.S., Delmelle, P., Stix, J., 2000. Passive degassing at Volcan Villarrica, south Chile. *Eos, Transactions of the American Geophysical Union* 81 (48) (Fall Meeting Supplement, Abstract V72C-03).
- Witter, J.B., Kress, V.C., Delmelle, P., HERSUM, T.G., 2001. Acid gas emissions measured by COSPEC, volatile trap, and filter pack at Volcan Villarrica, South Chile. *Eos, Transactions of the American Geophysical Union* 82 (47) (Fall Meeting Supplement, Abstract V42B-1012).